

Low-frequency spectra of bending wave turbulenceBenjamin Miquel *Université Paris-Saclay, CNRS, CEA, Service de Physique de l'État Condensé, 91191 Gif-sur-Yvette, France*

Antoine Naert

Laboratoire de Physique, Université Lyon, ENS de Lyon, Université Lyon 1, CNRS, F-69342 Lyon, France

Sébastien Aumaître*

*Laboratoire de Physique, Université Lyon, ENS de Lyon, Université Lyon 1, CNRS, F-69342 Lyon, France
and Université Paris-Saclay, CNRS, CEA, Service de Physique de l'État Condensé, 91191 Gif-sur-Yvette, France*

(Received 5 January 2021; accepted 4 May 2021; published 9 June 2021)

We study experimentally the dynamics of long waves among turbulent bending waves in a thin elastic plate set into vibration by a monochromatic forcing at a frequency f_o . This frequency is chosen large compared with the characteristic frequencies of bending waves. As a consequence, a range of conservative scales without energy flux on average exists for frequencies $f < f_o$. Within this range, we report a flat power density spectrum for the orthogonal velocity, corresponding to energy equipartition between modes. Thus, the average energy per mode β^{-1} —analogous to a temperature—fully characterizes the large-scale turbulent wave field. We present an expression for β as a function of the forcing frequency, amplitude, and of the plate characteristics.

DOI: [10.1103/PhysRevE.103.L061001](https://doi.org/10.1103/PhysRevE.103.L061001)

Introduction. Turbulence generically refers to physical systems where a large number of degrees of freedom exchange energy through nonlinear interactions and exhibit chaotic dynamics. A salient feature of these out-of-equilibrium systems is the existence of a scale separation between the characteristic scales of energy injection and of energy dissipation. From a phenomenological point of view, this scale separation permits energy cascades, a canonical example of which is the direct (i.e., down-scale) energy cascade in hydrodynamical turbulence (HT) between the (large) injection scale and the (small) dissipation scale [1,2]. From a theoretical point of view, this scale separation advocates for a statistical approach [3,4]. For instance, the Kolmogorov 1941 theory [5] (thereafter K41) captures successfully many statistical properties of the direct energy cascade in HT, although refined theories have been formulated later [3,4,6]. From a practical point of view, most numerical and experimental studies of hydrodynamic turbulence focus on this direct cascade and, therefore, consider fluid domains comparable to the forcing scale. However, larger structures might exist, provided that the system size allows for it. They have received much less attention, despite their relevance in many geophysical and astrophysical contexts [7]. A computationally savvy approach consists in modeling the large-scale modes only by considering the truncated Euler equation (e.g., Refs. [8,9]). These studies have recently established the generally accepted theoretical view that, in the absence of an energy flux through scales larger than the forcing scale, energy is statistically evenly distributed between these large scales [10–12]. This large-scale energy

equipartition is the hydrodynamic analogous to the thermal equilibrium.

Energy cascades are not exclusive to hydrodynamical turbulence but occur in other systems as well. For instance, cascades develop in a variety of nonlinear wave fields, which constitutes the focus of the present Letter. Similar to the hydrodynamical case, a statistical theory has been derived in the limit of weak nonlinearity: the weak wave turbulence theory (WWT) [13–15]. The most prominent success of the WWT is perhaps to derive analytically power-law spectra associated with a nonzero energy flux through scales ϵ . These spectra, coined Kolmogorov-Zakharov spectra, often take the form of power laws in both k and ϵ , the exponents of which depend on the nature of the interactions (dimensionality, number of interacting waves, dispersion relation, etc.). The theory has a wide range of applicability and has been successfully adapted to a variety of wave systems: gravity and capillary surface waves, sound waves, Alfvén waves, plasma waves, internal waves, nonlinear optics, Bose-Einstein condensates, and gravitational waves [13–16].

Among nonlinear interacting waves, we consider here the bending waves propagating in a thin elastic plate [17–19]. A turbulent spectrum has been proposed for the direct cascade in the WWT framework [20]. The prediction differs from experimental observations [21,22]. The discrepancy is attributed to the dissipation mechanisms [23,24]. The nonlinear interactions of elastic bending waves involves four waves but, in contrast to surface gravity waves, the number of waves in interaction is not necessarily conserved [20]. However, the existence of an inverse cascade (i.e., towards large scales) is still an open question. In Ref. [25], the authors observed an inverse cascade growing up during a transient regime. They

*Corresponding author: sebastien.aumaitre@cea.fr

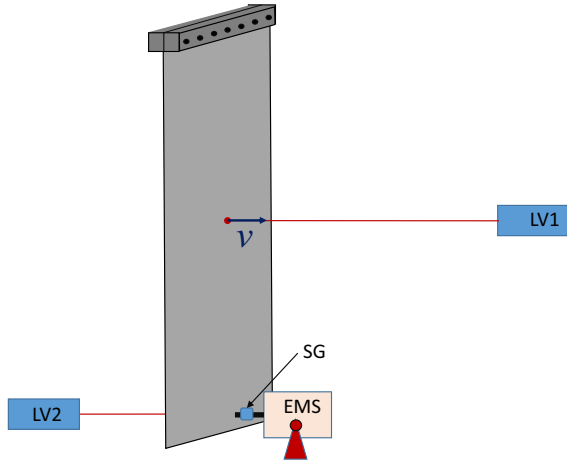


FIG. 1. Experimental setup: A thin stainless steel plate of ($2000 \times 1000 \times 0.5$ mm³) is forced by an electromagnetic shaker (EMS) at a frequency $f_o \in [100\text{--}300]$ Hz. The laser vibrometer (LV1) measures the velocity of the perpendicular deformation. In addition, we measure the force applied by the EMS with a strain gauge (SG) and the velocity at the injection point with a second laser vibrometer (LV2) (see the text).

attributed this transient inverse cascade to the interactions conserving the number of waves. In the numerical study of Ref. [25], the direct cascade is shrunk to a very short range in order to extend the inverse cascade. Moreover, the final stationary state is unknown.

Our aim in this Letter is to characterize experimentally the low-frequency spectrum of nonlinear bending waves in the stationary regime. The growth of the long wavelength has caught the attention of oceanographers for a long time and can be attributed partially to nonlinear interactions [26–28]. Laboratory experiments designed for such studies were performed only recently with surface gravity waves where an inverse cascade exists [29,30] and with capillary waves where no inverse cascade is expected for wavelengths smaller than the gravity-capillary crossover [31]. As we demonstrate below, flexion waves in thin steel plates prove a valuable candidate to study the large-scale dynamics of turbulent systems where one can easily excite and measure waves with temporal frequencies $1 \text{ Hz} \leq f \leq 300 \text{ Hz}$ (slower than the forcing) and with wavelength $1 \text{ cm} \leq \lambda \leq 100 \text{ cm}$.

Experimental device. Our experimental device is similar to the one presented in Ref. [32]. It is sketched in Fig. 1. A thin stainless steel plate ($2000 \times 1000 \times 0.5$ mm³) is forced with an EMS. In this setup, turbulent regimes are readily attained with a monochromatic forcing. Hence, we drive the shaker harmonically at a single frequency f_o , picked within the range from 100 to 300 Hz. We tested that broadband forcing (within a similar range) gives qualitatively similar results. The forcing point is at 10 cm from the bottom edge, and the top edge is clamped. All other boundaries are free. The low-frequency cutoff, f_c due to finite size of the plate is estimated with the dispersion relation of the bending waves: $2\pi f = chk^2$. Here f and k , respectively, are the bending wave frequency and wave number, h is the plate thickness, and c is a constant (with the dimension of a velocity) depending only on the mechanical properties of the plate materials [17].

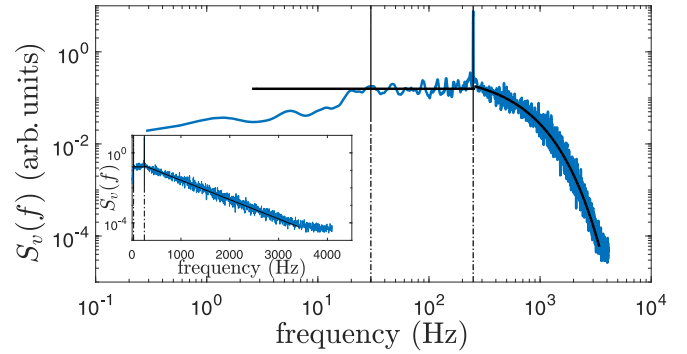


FIG. 2. PDS of the perpendicular velocity measured at a point in the middle of the plate with $f_o = 250$ Hz and an input power of 407 mW. The continuous black line represents the plateau value evaluated between 30 and 220 Hz. The main panel: The PDS is plotted with logarithmic axes. The inset: semilogarithmic axes are used. The vertical dot-dashed line points out the low-frequency cutoff at $f_c = 30$ Hz and the forcing frequency at $f_o = 250$ Hz.

In Ref. [22], the authors estimate $c = 1570$ m/s in a similar plate. Taking the cutoff wave number $k_c \sim 1/L$ with $L = 1$ m the plate width, one gets $f_c \sim 5$ Hz. In the following, we are interested in the spectra between f_c and f_o of the normal velocity v corresponding to displacements along the direction perpendicular to the plate at rest. This velocity is measured locally with LV1 near the center of the plate. We checked that the velocity spectrum does not depend on the exact position of the laser spot as long as it is 20 cm apart from the plate boundaries. LV2 measures the perpendicular velocity at the energy injection point where the EMS is attached to the plate. In addition, we measure the force applied by the EMS with a SG. The mechanical power injected into the nonlinear bending wave field, denoted I , is inferred from the product of these two measurements. In the next section, we present the low-frequency spectra of the perpendicular velocity v for various injected powers and driving frequencies. For each frequency and amplitude, we record the plate velocity for a quarter of an hour in the stationary regime. We probe each set of forcing parameters four times. The comparison of each four similar measurements gives us an estimate of the experimental reproducibility.

Experimental results. Figure 2 presents the power density spectrum (PDS) of the perpendicular velocity, S_v for a forcing frequency of $f_o = 250$ Hz and an input power of 407 mW. The forcing frequency remains clearly visible in the spectrum. Despite its amplitude, this peak actually contains only few percent of the total energy due to its narrowness. At frequencies higher than f_o , data are accurately fitted with an exponential decay $C(I, f_o) \exp(-\tau_o f)$, shown as the dashed line in the inset of Fig. 2. A similar exponential decay is found in the viscous range of hydrodynamic turbulence spectra [3,33]. Here τ_o is a characteristic decaying time, and $C(I, f_o)$ is a parameter depending on the forcing. This kind of decay holds for the entire range of driving parameters (I and f_o) explored in our experiment. Moreover, Fig. 3 shows that the characteristic time τ_o is, to a good approximation, inversely proportional to the rms velocity and independent of the forcing frequency, f_o , i.e., $\tau_o = \alpha/\sigma_v$ where α is a constant

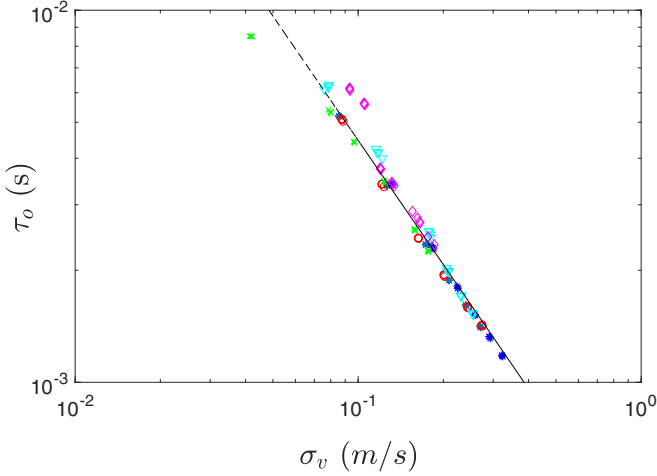


FIG. 3. The characteristic time of the exponential decay of the PDS of v as a function of the standard deviation of v . The various forcing frequencies are as follows: $f_o = 100$ Hz $*$, $f_o = 150$ Hz \circ (red), $f_o = 200$ Hz \times (green), $f_o = 250$ Hz \diamond (magenta), and $f_o = 300$ Hz ∇ (cyan). The dashed line represents the best fit of the experimental data. It gives an exponent of -1.1 ± 0.1 .

length independent of the forcing. From Fig. 3 one estimates: $\alpha \simeq 0.35$ mm.

Previous studies predict a power-law decay proportional to $f^{-\gamma}$ with $\gamma \approx 0.6$ followed by an exponential cutoff [21,22]. We do not observe such a universal power regime in our experiments. The discrepancy might be attributed to the higher forcing frequencies used in our experiment. This specific shape of the spectrum and the value of α is discussed in the next section. Despite the lack of a power-law cascade, we search for a signature of turbulence behavior by studying the scaling laws of the injected power I . More precisely, a signature of nonlinear energy transfer is that the energy flux $\epsilon \propto \langle I \rangle$ is proportional to the third moment of the v [23,34]. We confirm this scaling in Fig. 4. By comparing the range of the x axis of Figs. 3 and 4, we note that, despite being small, the skewness of the velocity field $\langle v^3 \rangle / \sigma_v^3$ is significantly nonzero. This minute deviation from Gaussianity is a necessary assumption of the WWT theoretical framework [13–15].

At frequencies lower than the forcing, i.e., $f < f_o$, the main panel of Fig. 2 shows a constant spectrum down to a cutoff frequency $f_c^{\text{obs.}} \sim 30$ Hz. This observed cutoff occurs at a frequency larger than our estimate based on the plate size L , which is $f_c(L) \sim 5$ Hz. However, it corresponds to a wavelength of nearly half the plate width $f_c(L/2) \sim 20$ Hz. It is not surprising that such low frequencies are affected by the sparse distribution of eigenmodes. We do not observe a dependency of $f_c^{\text{obs.}}$ with the forcing. This supports the assumption that this low-frequency cutoff is due to finite size effects [35]. To sum up our observation, for all forcing parameters explored in our experiment such that nonlinear waves are generated, we obtain the following picture: The temporal spectrum exhibits an exponential decay for $f > f_o$ and a plateau between f_c and f_o . The level of the plateau (shown by the continuous line in Fig. 2) does depend on the forcing parameters, though.

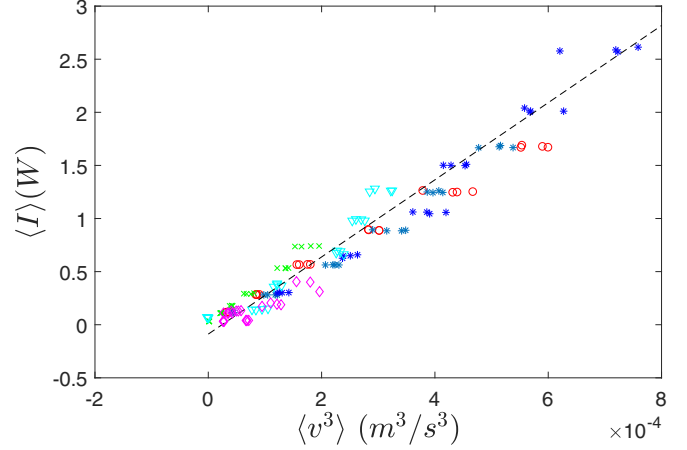


FIG. 4. The mean injected power $\langle I \rangle$ as a function of the third moment of the perpendicular velocity v . Symbols are as previously: $f_o = 100$ Hz $*$, $f_o = 150$ Hz \circ (red), $f_o = 200$ Hz \times (green), $f_o = 250$ Hz \diamond (magenta), and $f_o = 300$ Hz ∇ (cyan). The dashed line represents the best linear fit with a slope about 0.3 kg/m. The horizontal data scattering is due to the uncertainty on $\langle v^3 \rangle$ obtained from four identical experimental runs.

Discussions. In order to describe the shape of the spectrum shown in Fig. 2, we address the three following points.

(1) Scaling of the exponential decay for $f > f_o$. First, as a preliminary remark, we discuss the scaling of the exponentially decaying part of the spectra. Following Refs. [21,34], the dimensionless parameters are as follows:

$$\tilde{S}_v = S_v / (ch), \quad \phi = fh / \epsilon^{1/3}, \quad (1)$$

$$\phi_o = f_o h / \epsilon^{1/3}, \quad \xi = \epsilon / c^3. \quad (2)$$

We deliberately omit from this list the aspect ratio $\Gamma = h/L$ which has been kept constant. We recall that c is a characteristic velocity that depends on the material properties and ϵ (in m^3/s^3) is the mean energy flux by unit of mass injected in the two-dimensional waves. It is proportional to the mean injected power and quantifies the forcing intensity. If we denote $\phi = f/f^*$ with $f^* = \epsilon^{1/3}/h$, then f^* corresponds to the rescaling frequency previously introduced in Refs. [21,22]. Following Fig. 4, one has also: $f^* \propto \sigma_v/h$. From dimensional analysis, we seek a relation of the form $\tilde{S}_v = F(\phi, \phi_o, \xi)$, where F is an unknown function. We infer from Fig. 2 that $F(\phi, \phi_o, \xi)$ reduces to $\tilde{C}(\xi, \phi_o) \exp(-\tilde{\alpha}\phi)$ for all $f \geq f_o$ in the limit $f_o \gg f^*$. The length $\alpha \simeq 0.35$ mm, deduced from Fig. 3, is comparable to the thickness of the plate $h = 0.5$ mm. This observation supports the use of the dimensionless variable ϕ promoted in Ref. [21].

(2) Equipartition of energy for low-frequency modes $f < f_o$. We focus now on the low-frequency plateau. Energy is the unique conserved quantity during nonlinear interactions of bending waves [25]. In contrast to surface gravity waves in fluids, there is no other quantity (e.g. wave action) to sustain an inverse cascade. As a consequence, in the stationary regime, one assumes that there is no net energy flux through the lowest wave numbers, which contribute marginally to the overall dissipation [36]. It is, therefore, natural to expect equipartition of energy for these modes. With our data and the empirical

law for the dissipation presented in Ref. [23], we confirm that, at most, less than 10% of the power is dissipated below f_o (in the worst case, i.e., for $f_o = 300$ Hz). In the following, we will assume at first approximation that this has no influence on the low frequencies and does not perturb the measured plateau beyond the experimental uncertainty.

In order to explain the plateau, we now adapt the arguments exposed in Ref. [31] to the present case. We start with the two-dimensional isotropic energy spectral density per unit density and per unit surface. Once integrated over angles, one has: $e(k)dk = 2\pi k|\widehat{v}(k)|^2 dk$ where $\widehat{v}(k)$ is the Fourier transform of velocity. The equipartition of energy implies in a continuous limit (i.e., $k \gg 1/L$),

$$e(k)dk = \frac{1}{\beta} \frac{2\pi k dk}{(2\pi/L)^2} \frac{1}{\rho L^2} \Rightarrow e(k) = \frac{k}{2\pi\rho\beta}. \quad (3)$$

where ρ is the stainless steel density and β^{-1} is the typical energy per modes (analogous to a temperature). The power density spectrum of the perpendicular velocity is simply: $S_v(k) = e(k)/L$. Using the power density spectra relation $S_v(k)dk = S_v(f)df$ together with the dispersion relation, one gets

$$S_v(f) = \frac{1}{2\beta\rho cLh}. \quad (4)$$

In other words, the equipartition of energy corresponds to a flat frequency spectrum in agreement with the experimental spectrum at low frequency.

(3) Power spectra continuity hypothesis at $f = f_o$. The last step is to determine the variations of β with the driving parameters. As observations suggest, and despite the presence of a maximum in the spectrum at the forcing frequency that contains a negligible fraction of the total power, we match the low-frequency plateau and the direct cascade at the forcing frequency. We decompose the PDS into

$$S_v^<(f) = \frac{1}{2\beta\rho cLh} \quad \text{for } f \leq f_o, \quad (5)$$

$$S_v^>(f) = C \exp(-\tau_o f) \quad \text{for } f > f_o, \quad (6)$$

with $\tau_o \propto h/\sigma_v$ and where β and C are two unknown parameters whose value has yet to be determined. Neglecting the peak and the role of the frequency below f_c , in the energy spectrum, one requires that $S_v^<(f_o) = S_v^>(f_o)$ by continuity and that $\sigma_v^2 = \int_0^\infty S_v(f)df = \int_0^{f_o} S_v^<(f)df + \int_{f_o}^\infty S_v^>(f)df$. These two relations imply

$$C = \frac{\alpha\sigma_v^2}{\alpha f_o + \sigma_v} \exp(\alpha f_o/\sigma_v), \quad (7)$$

$$\beta^{-1} = 2\rho cL \frac{\alpha\sigma_v^2}{\alpha f_o + \sigma_v}. \quad (8)$$

Figure 5 shows that all the low-frequency plateaus are well rescaled by $S_v(f/f_o)(\alpha f_o + \sigma_v)/\sigma_v^2$ and that β^{-1} is a linear function of $\sigma_v^2/(\alpha f_o + \sigma_v)$. Moreover, from Fig. 4 one expects $\sigma_v \sim I^{1/3}$. Thus, one writes β^{-1} as a function of the forcing parameters: $\beta^{-1} \sim 2\rho cL(\alpha I^{2/3})(\alpha f_o + I^{1/3})$. Note that the ratio $\alpha f_o/\sigma_v$ is on the order of one. Thus, Eqs. (7)

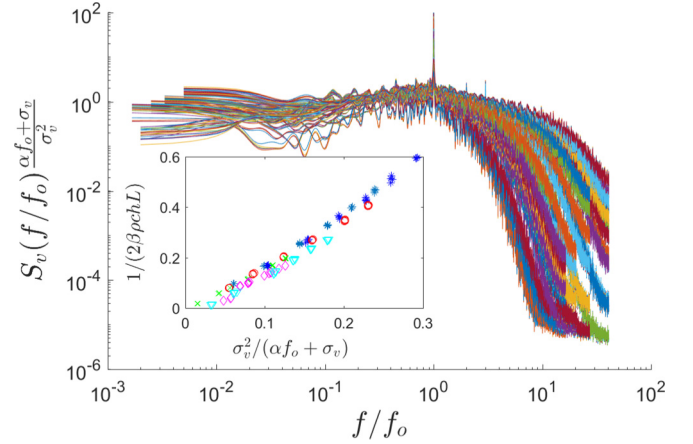


FIG. 5. Collapse at low frequency ($f \leq f_o$) of S_v , the PDS of the perpendicular velocity of the plate, once rescaled by the expected plateau value: $\sigma_v^2/(\alpha f_o + \sigma_v)$ as a function of the reduced frequencies f/f_o for all the 156 experimental runs. The inset: linear relation between the plateau value and $\sigma_v^2/(\alpha f_o + \sigma_v)$ with the forcing frequency: $f_o = 100$ Hz *, $f_o = 150$ Hz \circ (red), $f_o = 200$ Hz \times (green), $f_o = 250$ Hz \diamond (magenta), and $f_o = 300$ Hz ∇ (cyan).

and (8) cannot be simplified further in our range of forcing parameters.

Concluding remarks. In sum, bending waves forced in a thin elastic plates prove a useful setup to explore the low-frequency spectrum of turbulent systems in the absence of an inverse cascade. We observe in this system that mean energy is evenly distributed between modes. Finally, we propose an expression allowing a full characterization of the low-frequency part of the velocities spectrum knowing the injected power and the forcing. The buildup of this equipartition possibly occurs through a transient inverse cascade as reported in Ref. [25]. An experimental study of the transient associated with high-frequency forcing would be a challenging endeavor to generalize previous studies of direct cascade transients in elastic plates [37]. In practice, leveraging a space and time measure of the deformation, one could analyze the time evolution of the spatial modes. The variations of this mean energy per mode β^{-1} with the forcing parameters is obtained by assuming the continuity of the spectrum. Ideally, one would aim at observing simultaneously energy equipartition for low-frequencies $f \leq f_o$ and a direct cascade (characterized by a power-law spectrum) for $f \geq f_o$, before dissipative effects take over. In the present experiment, high driving frequencies were necessary so that equipartition was observed over a convincingly large range of frequencies. As an unfortunate consequence, the small scales did not exhibit conservative cascades but were affected by dissipation. A goal for future studies, perhaps achievable using a much larger plate, would be to somehow extend the range of the “transparency window” (i.e., the range of scales where energy is conservatively transferred) so that to observe simultaneously equipartition and a direct cascade that is ultimately dissipated at small scales.

Acknowledgments. This work was supported by the French National Research Agency (ANR DYSTURB Project No. ANR-17-CE30-0004). We would like to thank G. Michel, S. Fauve, and B. Gallet for helpful discussions.

- [1] L. Richardson, *Weather Prediction by Numerical Process* (Cambridge University Press, Cambridge, UK, 1922).
- [2] A. Alexakis and L. Biferale, *Phys. Rep.* **767-769**, 1 (2018).
- [3] A. S. Monin and A. M. Yaglom, in *Statistical Fluid Mechanics, Mechanics of Turbulence*, edited by J. L. Lumley (MIT Press, Cambridge, MA, 1981), Vol. 2.
- [4] U. Frish, *Turbulence: The Legacy of A. N. Kolmogorov* (Cambridge University Press, Cambridge, UK, 1995).
- [5] A. N. Kolmogorov, Dokl. Akad. Nauk SSSR [Sov. Phys. Dokl.], **30**, 9 (1941).
- [6] A. N. Kolmogorov, *J. Fluid Mech.* **13**, 82 (1962).
- [7] F. Bouchet and A. Venaille, *Phys. Rep.* **515**, 227 (2012).
- [8] V. Dallas, S. Fauve, and A. Alexakis, *Phys. Rev. Lett.* **115**, 204501 (2015).
- [9] A. Alexakis and M.-E. Brachet, *J. Fluid Mech.* **884**, A33 (2020).
- [10] P. G. Saffman, *J. Fluid Mech.* **27**, 581 (1967).
- [11] R. H. Kraichnan, *J. Fluid Mech.* **59**, 745 (1973).
- [12] H. A. Rose and P. L. Sulem, *J. Phys. (Paris)* **39**, 441 (1978).
- [13] V. E. Zakharov, V. S. L'vov, and G. Falkovich, *Kolmogorov Spectra of Turbulence 1: Wave Turbulence* (Springer, Berlin, 1992).
- [14] A. C. Newell, B. Rumpf, *Annu. Rev. Fluid Mech.* **43**, 59 (2011).
- [15] S. Nazarenko, *Wave Turbulence*, Lecture Notes in Physics Vol. 824 (Springer-Verlag, Berlin/Heidelberg, 2011).
- [16] S. Galtier and S. V. Nazarenko, *Phys. Rev. Lett.* **119**, 221101 (2017).
- [17] L. Landau and E. Lifshitz, *Theory of Elasticity* (Pergamon Press, New York, 1959).
- [18] M. Amabili, *Nonlinear Vibrations and Stability of Shells and Plates* (Cambridge University Press, Cambridge, UK, 2008).
- [19] B. Audoly and Y. Pomeau, *Elasticity and Geometry: From Hair Curls to the Nonlinear Response of Shells* (Oxford University Press, Oxford, 2010).
- [20] G. Düring, C. Josserand, and S. Rica, *Phys. Rev. Lett.* **97**, 025503 (2006).
- [21] N. Mordant, *Phys. Rev. Lett.* **100**, 234505 (2008).
- [22] A. Boudaoud, O. Cadot, B. Odille, and C. Touzé, *Phys. Rev. Lett.* **100**, 234504 (2008).
- [23] T. Humbert, O. Cadot, G. Düring, C. Josserand, S. Rica, and C. Touzé, *Europhys. Lett.* **102**, 30002 (2013).
- [24] B. Miquel, A. Alexakis, and N. Mordant, *Phys. Rev. E* **89**, 062925 (2014).
- [25] G. Düring, C. Josserand, and S. Rica, *Phys. Rev. E* **91**, 052916 (2015).
- [26] H. Mitsuyasu, *J. Oceanogr.* **58**, 109 (2002).
- [27] L. Romero and W. K. Melville, *Phys. Oceanogr.* **40**, 441 (2010).
- [28] V. E. Zakharov, S. I. Badulin, P. A. Hwang, and G. Caulliez, *J. Fluid Mech.* **780**, 503 (2015).
- [29] L. Deike, C. Laroche, and E. Falcon, *Europhys. Lett.* **96**, 34004 (2011).
- [30] E. Falcon, G. Michel, G. Prabhudesai, A. Cazaubiel, M. Berhanu, N. Mordant, S. Aumaître, and F. Bonnefoy, *Phys. Rev. Lett.* **125**, 134501 (2020).
- [31] G. Michel, F. Pétrélis, and S. Fauve, *Phys. Rev. Lett.* **118**, 144502 (2017).
- [32] B. Apffel, A. Naert, and S. Aumaître, *J. Stat. Mech.* (2019) 013209.
- [33] R. H. Kraichnan, *J. Fluid Mech.* **5**, 497 (1959).
- [34] C. Connaughton, S. Nazarenko, A. C. Newell, *Physica D* **184**, 86 (2003).
- [35] B. Miquel, A. Alexakis, C. Josserand, and N. Mordant, *Phys. Rev. Lett.* **111**, 054302 (2013).
- [36] V. Lvov, H. Andy, and G. V. Kolmakov, *Europhys. Lett.* **112**, 24004 (2015).
- [37] B. Miquel and N. Mordant, *Phys. Rev. Lett.* **107**, 034501 (2011).